Bull Volcanol (2001) 63:345–359
DOI 10.1007/s004450100150

RESEARCH ARTICLE

D. M. Palladino · M. Gaeta · F. Marra

A large K-foiditic hydromagmatic eruption from the early activity of the Alban Hills Volcanic District, Italy

Received: 30 July 2000 / Accepted: 21 April 2001 / Published online: 5 July 2001

Abstract In this paper we discuss the uncommon case of an energetic, pyroclastic-flow-forming eruption with a SiO_2-poor (42–45 wt.%), K-foiditic magma composition. The Trigoria-Tor de' Cenci Tuff (TTC; 561 ka) is the product of the first large-scale explosive event (of the order of 1–10 km^3 of erupted products) in the Alban Hills Volcanic District, near the city of Rome, Italy. After an initial Plinian phase that produced a scoria fall horizon, pyroclastic current activity emplaced ash deposits with leucite-bearing juvenile scoria lapilli. The abundance of accretionary lapilli, the most distinctive feature of these deposits, together with the high degree of fragmentation, the abundance of minute lithic inclusions and the morphology of ash particles, indicates a hydromagmatic character for the most part of the eruption. The absence of vent-derived carbonate lithic clasts from the deep regional aquifer and the abundance of cognate lithic fragments suggest that the interaction with external water involved a surficial aquifer in the older Alban Hills volcanic terrains. Perhaps the most striking aspect of the TTC is the K-foiditic composition of the pre-eruptive melt, which, to our knowledge, is unique among explosive events of comparable size elsewhere in the world. The pre-eruptive magma system feeding the TTC was controlled mainly by leucite+clinopyroxene fractionation under $a_{H2O}<1$ conditions. The low SiO_2 activity prevented plagioclase and K-feldspar crystallization. The depth of the magma chamber can be estimated at 3–6 km within the carbonate substrate. In contrast to the other major pyroclastic-flow-forming eruptions of the Alban Hills, the juvenile volatile exsolution due to magma crystallization is not seen as the main mechanism driving the TTC eruption. We suggest that the explosive behaviour of the TTC magma in the early magmatic phase resulted from a rapid decompression due to a regional seismic event and from magma–water interaction in the succeeding phase.

Keywords Explosive eruption · Hydromagmatism · Pyroclastic deposit · Pyroclastic current · Potassic volcanism · K-foidite · Alban Hills

Editorial responsibility: T.H. Druitt

D.M. Palladino (✉) · M. Gaeta
Dipartimento di Scienze della Terra, Università "La Sapienza",
P.le A. Moro 5, 00185 Rome, Italy
e-mail: danilo.palladino@uniroma1.it
Tel.: +39-06-49914916, Fax: +39-06-4454729

F. Marra
Istituto Nazionale di Geofisica e Vulcanologia,
Via di Vigna Murata 605, 00143 Rome, Italy

Introduction

The city of Rome lies between the two Quaternary potassic volcanic districts of the Sabatini Mounts to the NW and the Alban Hills to the SE (Fig. 1), whose contemporaneous activities have characterized the geological history of the area over the past 0.6 Ma. The fortune of the "eternal city" itself, since its birth on the Palatine Hill, was greatly enhanced by the favourable geological context set by the volcanic relief of the famous seven hills facing the Tiber River. The first large-scale explosive eruption in the Alban Hills, and the main subject of this paper, emplaced the "Trigoria-Tor de' Cenci Tuff" (TTC), which is part of those pyroclastic deposits of the Roman area known in the literature as "Tufi pisolitici" (Fornaseri et al. 1963). Typically this name has been used in general to indicate several ash deposits, rich in accretionary lapilli ("pisoliti"), emplaced during the early phases of activity of the Alban Hills and the Sabatini Mounts. Fornaseri et al. (1963) named "Tufo Grigio Pisolitico" (grey pisolitic tuff) a specific volcanic unit of the Alban Hills, which broadly corresponds to the Tuscolano-Artemisio "first pyroclastic flow unit" of De Rita et al. (1988). However, Marra and Rosa (1995) recognized at least two eruptive events producing pyroclastic flow deposits with accretionary lapilli during the early Alban Hills activity, namely the "Tor de' Cenci" and "Palatino" units. The older Tor de' Cenci unit, called "Tufo Pisolitico di Trigoria" by Karner et al. (2001a),

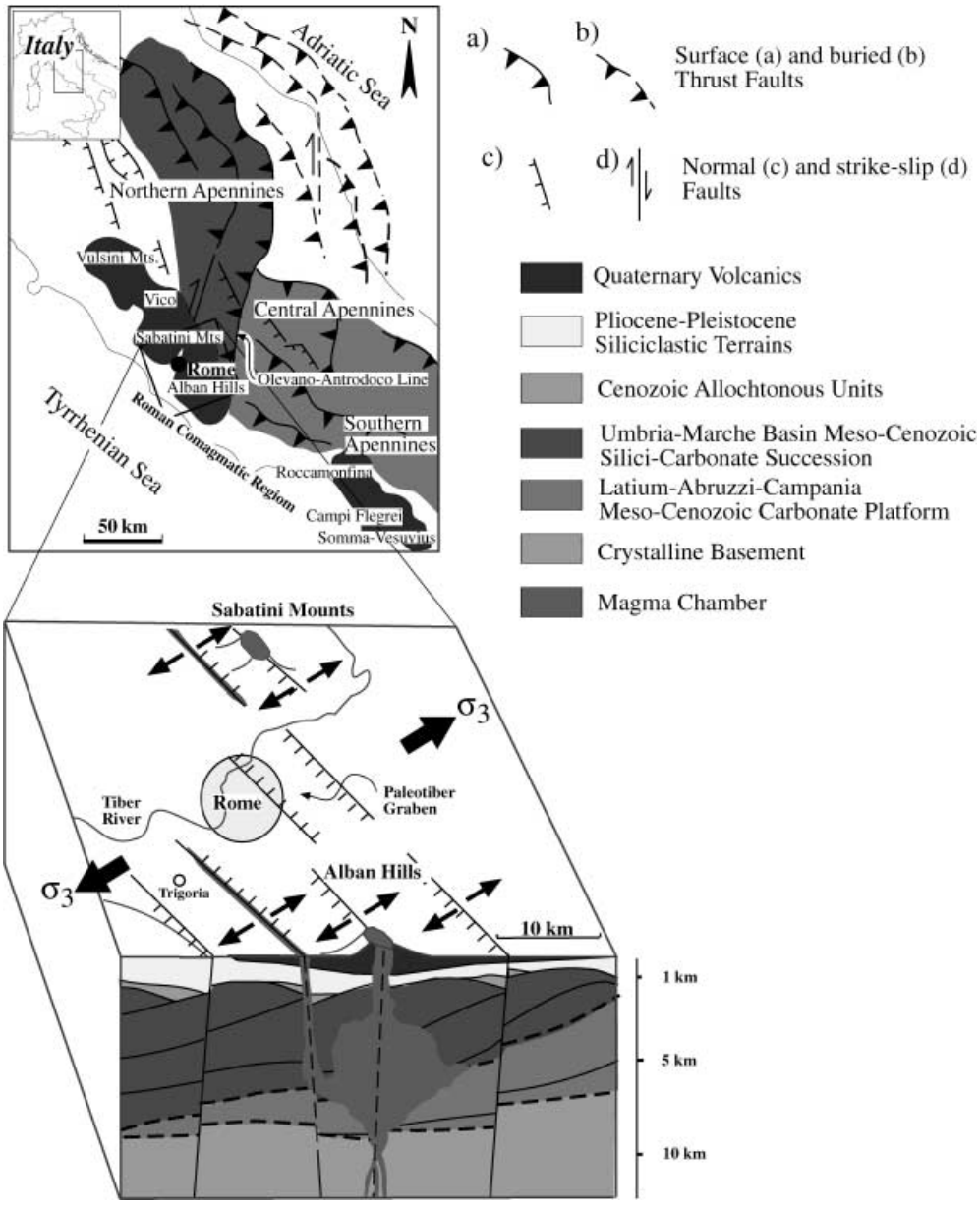

Fig. 1 Geologic sketch map of central Italy showing the main volcanic and regional tectonic features and enlarged tectonic sketch of the Roman area with a schematic cross section showing the lithologies of the substrate beneath the Alban Hills

corresponds with the TTC. Considering that the most favourable and complete exposure is preserved near the locality of Trigoria, south of Rome (Fig. 1), and to avoid confusion with the past literature, we retain here both previous names.

In the present work we define the complete eruptive succession of the TTC and propose an interpretation of eruptive and emplacement processes. We also report chemical, mineralogical and petrographic characteristics of the erupted products and then present a petrological model of the pre-eruptive magma system. In a wider context, this contribution improves our knowledge of the unusual magmatic system of the Alban Hills during the initial stage of volcanic activity. To explain the highly explosive character of the eruption, coupled with the SiO_2-poor, K-foiditic magma composition, we suggest a regional seismic trigger and hydromagmatism as possible causes.

Geological setting

The Alban Hills belong to the Roman Comagmatic region (Washington 1906), a NW/SE-trending chain of potassic volcanoes that developed along the Tyrrhenian margin of central Italy during Middle Pleistocene. Recent studies (Serri et al. 1991) have interpreted the volcanic activity in the northern-central Tyrrhenian Sea basin (starting at ca. 14 Ma) as back-arc volcanism, consequent to NE–SW extensional tectonics at the rear of the Apennine thrust-and-fold belt induced by the NE retreat of a subducting slab (Malinverno and Rayan 1986; Patacca et al. 1991). Extensional tectonics has affected the Tyrrhenian margin of Italy since Messinian, causing the collapse of the carbonate structures of the Apennine and the opening of NW–SE elongated basins that were filled by a succession of marine sediments up to 2000 m

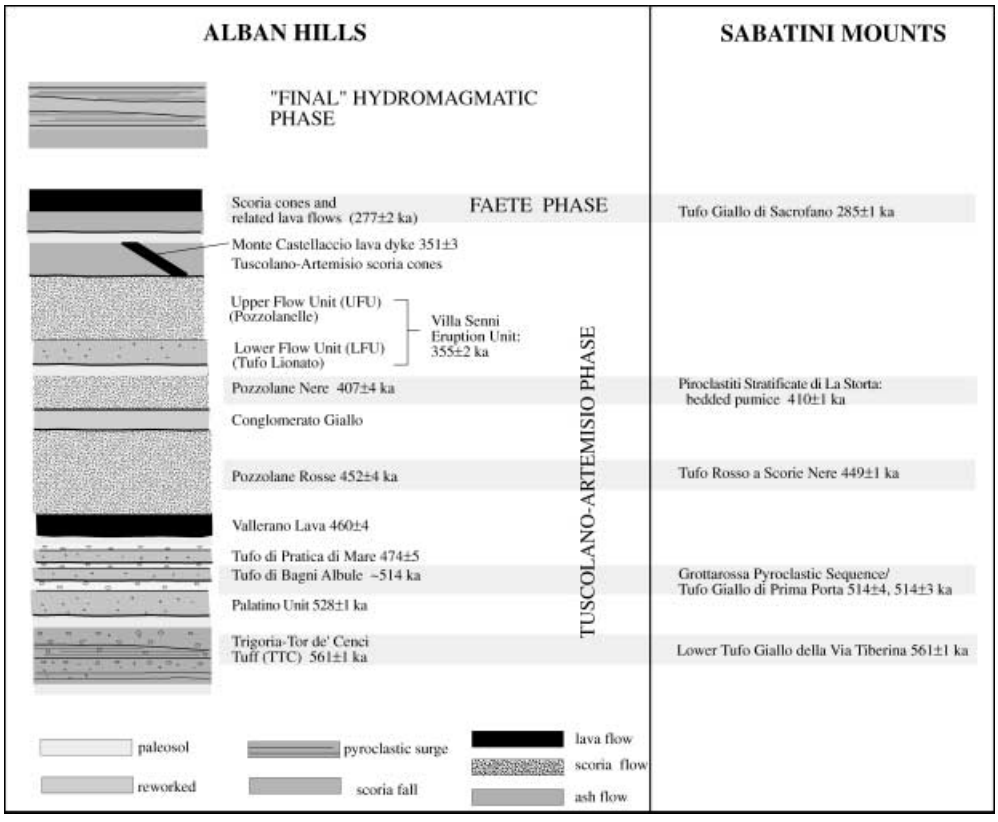

Fig. 2 Stratigraphic and geochronological scheme of the Alban Hills activity. The main eruptive events of the Sabatini Mounts are reported for comparison. The $^{40}Ar/^{39}Ar$ dates are from Karner et al. (2001a). Even taking into account the analytical errors on the dates, considering that the repose times among large-volume eruptions in the two districts are of the order of 10^4 years, the parallelism in the eruption timing is striking, suggesting a regional tectonic control

thick throughout Pliocene and early Pleistocene (Marra et al. 1995). The progressive upswelling of this area since the early Pleistocene was probably driven by the injection of magma into the upper crust induced by extension-related thinning, leading to the opening of magma conduits and the start of volcanism at around 800 ka (Karner et al. 2001a).

The volcanic districts of the Alban Hills and the Sabatini Mounts are rooted on structural highs of the carbonate substrate (Funiciello and Parotto 1978; De Rita et al. 1993). In particular, the Alban Hills district developed at the rear of the southern continuation of the Olevano-Antrodoco line, a north-striking thrust front across which the Umbria-Marche Basin tectonic unit of the Apennine Chain thrusts eastward over the Latium-Abruzzi-Campania Carbonate Platform (Funiciello and Parotto 1978), resulting in overthickened carbonate bedrock (Fig. 1).

As detailed geochronology shows (Karner and Renne 1998; Karner et al. 2001a), the two districts had parallel eruptive histories (Fig. 2). Although volcanic activity since 802±4 ka has been documented in the Sabatini Mounts (and probably in the Alban Hills), the main period of explosive activity started contemporaneously in the two districts at 561±1 ka (Lower "Tufo Giallo della Via Tiberina" from the Sabatini Mounts and TTC eruptions) and lasted until ~280 ka, with remarkably synchronous, large eruptive events (including the largest of the two districts, i.e. the "Tufo Rosso a Scorie Nere" from the Sabatini Mounts and the "Pozzolane Rosse" from the Alban Hills).

Different authors have suggested a strong regional structural control over the Roman volcanoes (Locardi et al. 1977; Faccenna et al. 1994; Marra 2001). A NW–SE elongated graben developed in the area of Rome (Palaeotiber Graben; Fig. 1; Marra et al. 1998), as a consequence of a climax of NE–SW extensional tectonics (Karner et al. 2001b), concurrent with the start of volcanism. Karner et al. (2001b), by comparing the tectonic history of the Tyrrhenian margin of the Roman area with the volcanic history of the Sabatini Mounts and the Alban Hills, have found a strong link among tectonic and volcanic phases and have suggested that some of the largest eruptions were triggered by increased rates of extension. In fact, as documented from coastal terrace elevation, two major pulses of uplift coincide with increased extensional tectonics in the inland area. These events herald the start of the volcanic activity in the Sabatini Mounts (and probably in the Alban Hills) at ~800 ka and the main explosive phases of both volcanoes at ~600 ka.

The essential features of the Alban Hills district comprise an old main stratovolcano, truncated by the Tuscolano-Artemisio caldera in the central area, with the Faete edifice inside it and a cluster of younger eccentric tuff rings to the west (Fig. 3). Hydrogeological studies indicate the presence of a shallow aquifer located within the Alban Hills volcanics and a deep regional aquifer in the

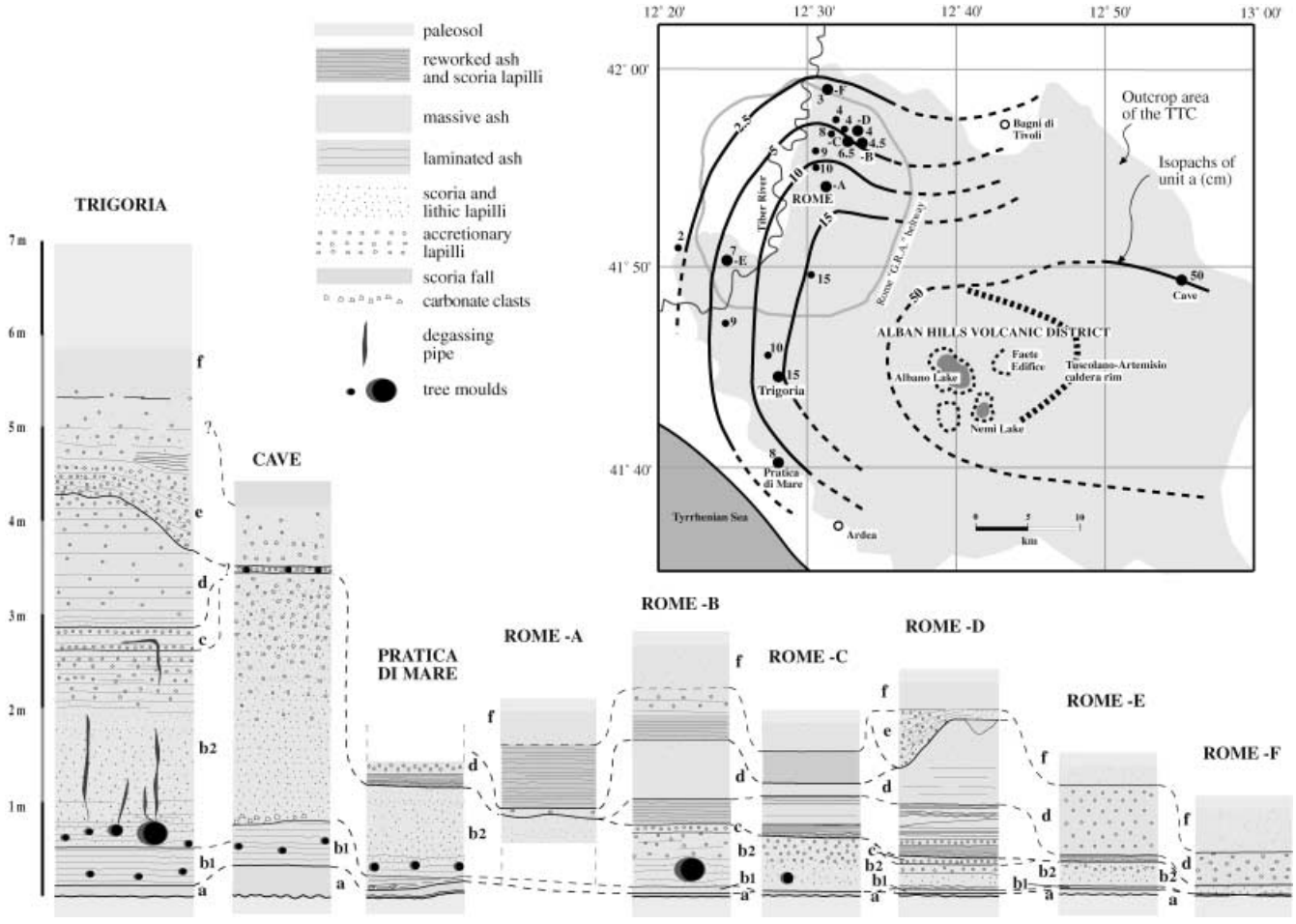

Fig. 3 Stratigraphic logs of the Trigoria-Tor de' Cenci Tuff (TTC). *Lower-case letters* beside stratigraphic logs refer to the depositional units described in the text. *Top right inset*: sketch map of the outcrop area of the TTC, showing the location of the stratigraphic logs and thicknesses (in centimetres) of the basal scoria fall deposit (unit a)

Meso-Cenozoic carbonates, separated by low-permeability siliciclastic and marly terrains (aquiclude) of Plio-Pleistocene (Boni et al. 1995). The top of the carbonate substrate is located at a depth of ~1 km under the Tuscolano-Artemisio caldera floor, in the central area of the Alban Hills (Fig. 1).

Stratigraphic position and absolute age of the TTC

Generally, the products of the TTC eruption rest on top of an immature palaeosol developed on ash deposits (with pumice and accretionary lapilli) that we ascribe to the early activity of the Sabatini Mounts, and reworked volcaniclastic horizons overlying continental sand-gravel deposits of the "Ponte Galeria" Formation (Middle Pleistocene; Marra et al. 1998).

The TTC is the stratigraphically lowest exposed product of the volcanic activity in the Alban Hills district, although the occurrence of lava and tuff inclusions in the TTC itself documents earlier activity in the central area of the district. The TTC eruption is the oldest of the five major explosive eruptions of the early phase of activity of the Alban Hills (called Tuscolano-Artemisio phase; Fig. 2) and is therefore interpreted as marking the onset of large-scale explosive activity in the district. The Tuscolano-Artemisio phase was by far the most important, in terms of eruption intensities and magnitudes, of the three phases of activity recognized in the district, and emplaced at least 283 km^3 of products (De Rita et al. 1995) in the time span ~560–350 Ma. Toward the end of this phase the "Villa Senni" eruption (Freda et al. 1997) took place and the Tuscolano-Artemisio caldera formed.

The $^{40}Ar/^{39}Ar$ age of the TTC determined on leucite crystals from subunit b1 sampled at Trigoria (Fig. 3) is 561±1 ka (Karner et al., 2001a), which is in good agreement with that previously determined on leucite from a distal portion of the same unit (557±15 ka; Karner and Renne 1998). It is noteworthy that the radiometric age of the TTC is indistinguishable from that obtained for the first major eruption of the Sabatini Mounts, the Lower Tufo Giallo della Via Tiberina (561±1 ka; Karner et al., 2001a). In most localities, a decimetre- to >1-m-thick palaeosol separates the TTC from the overlying Palatino unit (528±1 ka) of the Tuscolano-Artemisio.

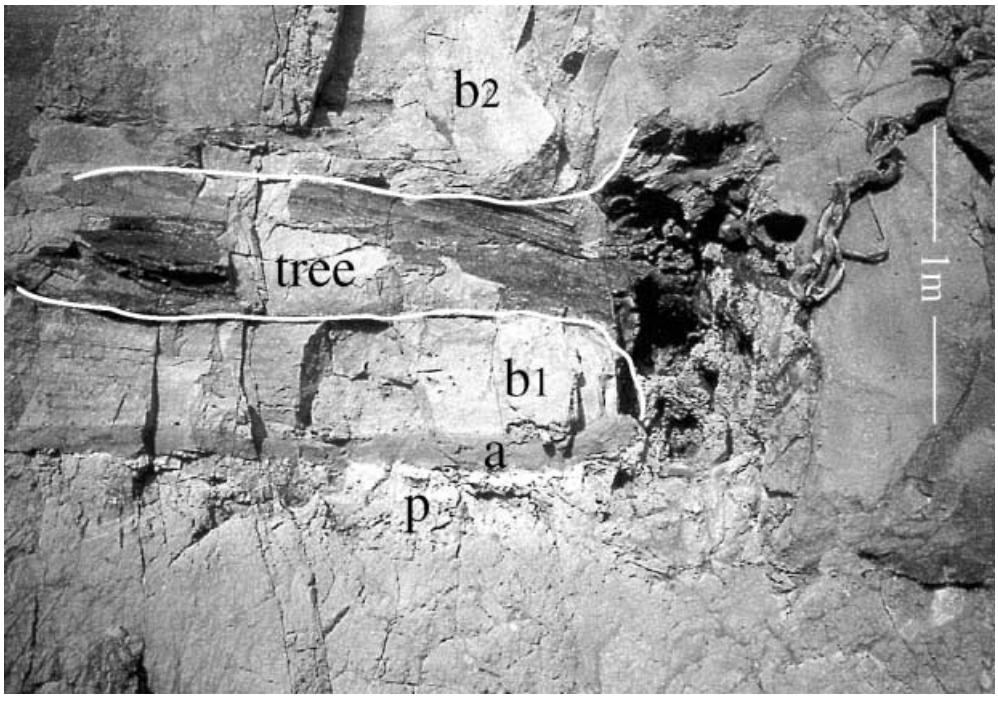

Fig. 4 Trigoria locality: lower part of the TTC eruptive succession (p=palaeosol) showing a large uprooted tree. The bending of unit a and subunit b1 deposits on the right-hand side of the photograph suggests that the tree log fell down after deposition of unit a and subunit b1, and then was uprooted, but not dragged away, by the passage of the pyroclastic current which emplaced subunit b2. The E–W strike (i.e. from right to left) of the fallen tree and the position of the roots clearly indicate that the pyroclastic current travelled westward at this location, consistent with the inferred vent area

Areal distribution and depositional features

The TTC crops out mainly in the western sector of the Alban Hills over an area in excess of 1000 km^2 (Fig. 3). It is generally exposed in relatively distal settings, whereas in proximal ones it is buried under the thick younger volcanic succession. In particular, it is widely recognized in the entire metropolitan area of Rome, and as far south as Ardea. Scattered outcrops are also found to the east (e.g. "Bagni di Tivoli", "Cave"), suggesting an almost axisymmetrical distribution around a probable vent in the area of the present-day Tuscolano-Artemisio caldera. On the basis of the inferred areal distribution and average thickness of a few metres, a conservative estimate of the total volume of erupted products is of the order of 1–10 km^3.

At the reference section of Trigoria, six depositional units have been recognized, which are broadly correlatable through the outcrop area. These are described below from bottom to top (Fig. 3).

Unit a, 15 cm thick at Trigoria, is made up of a well sorted, clast-supported bed of dark-grey, angular scoria lapilli that mantles the pre-eruption substrate. These depositional features are clearly indicative of a fallout origin. Scoria clasts are generally millimetre-sized and normally graded, except in the topmost inversely graded interval, where they reach 1 cm in size. Unit a crops out extensively to the west of the Alban Hills, whereas it is rarely exposed to the east. It thins radially from the central area of the Alban Hills to a few centimetres in the western sector and appears to attain a maximum of 50 cm in the eastern sector (i.e. at Cave; Fig. 3). Although the paucity of exposures in the eastern sector does not allow a detailed location of the eruptive vent, it is inferred that the dispersal axis broadly trends eastward or southeastward, as for the other major scoria fall deposits of the Tuscolano-Artemisio (unpublished data of the authors). Thus, in contrast to what is commonly observed in pyroclastic fall deposits, it seems that unit a mostly crops out upwind (i.e. NW), rather than downwind, of the eruption column. Accordingly, the Inman's grain-size parameters show that unit a is coarser grained at Cave (Md_ϕ=–0.05), relative to Pratica di Mare to the SW (Md_ϕ=+1.05) and less sorted at Pratica di Mare (σ_ϕ=1.13 vs 0.68 at Cave) due to higher ash content.

A 0.5-cm-thick, well-sorted, coarse ash layer containing remnants of uncharred leaves marks the base of unit b and can be traced to the SW of the Alban Hills, as far as Pratica di Mare (Fig. 3). Unit b comprises a light-grey, indurated, ash horizon 40–50 cm thick (subunit b1), grading upward into a coarser 190-cm-thick, indurated, grey-tawny ash matrix-supported deposit (subunit b2) containing altered leucite and abundant millimetre- or, rarely, centimetre-sized grey scoria lapilli and lava and tuff inclusions. Repeated slight grain-size variations and/or laterally discontinuous trails of fine lapilli impart a centimetre-scale lamination to the lower subunit (b1), indicative of late-stage tractional transport, while the main body (b2) has a massive appearance, except for a crude inverse grading of scoria and lithic lapilli in the lower half. Up to centimetre-sized accretionary lapilli, made up of ash coating crystal or lithic fragments, are present and become very abundant in the upper part. Of note is the common occurrence of vegetation casts, up to a few centimetres in diameter, with uncharred wood in b1, and of tree moulds, up to a few decimetres in diameter, with incipiently carbonized wood in b2 (Fig. 4). Fines-poor degassing pipes originate from tree moulds and extend upward for up to 1 m, indicating prolonged

heating and drying of incorporated wood after deposition. The proportion of millimetre-sized grey scoria and lithic clasts significantly decreases from medial (e.g. Rome-A; Fig. 3) to more distal (Rome-B-C-D) settings. In the western sector, thickness is observed to decrease with increasing distance from the central area of the Alban Hills (Fig. 3). The partition into laminated subunit b1 and massive, accretionary lapilli-bearing, subunit b2 (up to 50 cm and 3 m thick, respectively) is also recognizable to the east (e.g. Cave). Tree moulds, up to 1 dm in diameter, well-preserved reeds, and centimetre-sized, locally derived, carbonate clasts from the pre-eruptive ground surface at the base of subunit b2 are prominent features in this sector.

Unit b grades upwards into a 25- to 70-cm-thick ash horizon (unit c) containing millimetre-sized lithic fragments and swarms of accretionary lapilli in the lower part and abundant accretionary lapilli in the upper part. Vertical degassing pipes, rich in accretionary lapilli and minute scoria and lithic fragments, are observed to originate from subunit b2, to cross the b2/c boundary and to extend some centimetres within unit c. Generally, a sharp, flat contact separates unit c and overlying unit d. An intervening laminated horizon of coarse ash of probable deposition by running water marks the boundary between units c and d in more distal sites (e.g. Rome-B-C-D; Fig. 3).

Unit d, up to 130 cm thick, consists of an indurated fine-ash deposit, with a decimetre-scale bedding imparted by discontinuous trails of accretionary lapilli, topped by a distinctive, 30-cm-thick, bed of accretionary lapilli and interstitial ash. Minute scoria and lithic fragments are far less abundant than in the enclosing units. Individual beds appear either massive or planar- to cross-laminated, with rhythmic grain size variations (commonly defined by trails of minute accretionary lapilli) even on a millimetre scale. In more distal sites (e.g. Rome-B-C-D; Fig. 3), unit d consists of a well-sorted aggregate of millimetre-sized grey scoriae and altered leucite crystals with a laminated texture. In the eastern sector (e.g. Cave), it can be correlated with a 5-cm-thick ash horizon, rich in accretionary lapilli and small uncharred branches, resting on top of unit b.

Unit e, which unconformably overlies unit d, is a tawny, ash-matrix-supported, indurated deposit, up to 120 cm thick, with abundant accretionary lapilli, grey to yellowish fine scoria lapilli and altered leucite crystals. The sharp erosional d/e contact observed at the type locality can be identified in the Rome area where unit e is channelled in places (e.g. Rome-D; Fig. 3). In other cases (Rome-A-B-C; Fig. 3), decimetre-thick, laminated, coarse ash deposits rich in altered leucite are the reworked equivalent of unit e.

Unit f, a 30-cm-thick, massive, ash deposit, containing yellowish, millimetre-sized scoria clasts, closes the TTC eruptive succession and passes upward to a reddish-brown palaeosol, up to 110 cm thick. Unit f and associated palaeosol have minor variations in thickness, texture, grain size and componentry through the study area.

Millimetre-sized lithic fragments of grey lavas and subordinate yellow tuffs, including leucite+sanidine-bearing rock types (mostly from units b and e), provide the only available information up to now on the pre-TTC volcanic substrate in the Alban Hills area. Conversely, vent-derived siliciclastic and carbonate lithic clasts from deeper country rocks are quite rare throughout the TTC succession.

Eruption and emplacement processes

The fine grain size (and consequent lack of information from the grading pattern of coarse clasts) and induration (which prevents detailed grain-size studies) of most of the TTC deposits rendered the reconstruction of related transport and depositional processes problematic.

As is typical of major explosive eruptions of Tusculano-Artemisio, the TTC eruption started with the fallout of poorly vesicular scoria clasts rather than true pumice. The width of the areal distribution of unit a (Fig. 3) reasonably implies deposition from a sustained eruption column. The paucity of thickness data in the eastern sector prohibits classification of the event in terms of dispersal vs fragmentation parameters (Walker 1973). However, from the maximum thickness of 2 m, which can be extrapolated on a semilogarithmic thickness–distance plot (not reported), it can be inferred that the area enclosed by the 1/100 of maximum thickness isopach (i.e. the 2 cm isopach) is well beyond the lower limit of the Plinian field in the Walker's (1973) classification scheme. The obtained thickness–half distance parameter of 5–6 km is also compatible with a Plinian event (Pyle 1989). Moreover, from the available isopachs and the observed thickness of 50 cm as far as Cave (Fig. 3), it is deduced that the areal extent and volume of products (in the range 0.1–1 km^3) are broadly comparable with the scale of other Plinian events of the Roman Province (Palladino and Agosta 1997, and unpublished data).

The ash layer with uncharred leaves overlying unit a records the passage of an early pyroclastic surge pulse, heralding the pyroclastic current activity that formed unit b. Since facies relationships in this unit are not exposed in proximal areas, we cannot assess an origin of subunit b1 either by an independent surge episode or by possible ash cloud surge detachment from, and deposition ahead of, the more concentrated part of the pyroclastic current emplacing subunit b2, as proposed for Merapi volcano (Bourdier et al. 1997). However, the gradational contact with subunit b2, and the overall coarsening upward of transported pyroclasts (and trees), indicate increasingly energetic conditions within nearly continuous flow activity. Therefore it is more likely that b1 and b2 reflect gradually changing emplacement regimes, rather than distinct flow episodes.

The massive appearance, inverse grading and general textural features of subunit b2, as well as the enclosed tree logs, suggest a high deposition rate from a high-particle concentration, likely laminar, pyroclastic current.

The presence of partly carbonized wood on the outer surface of tree logs allow us to estimate the emplacement temperature of the enclosing flow at around 250°C, corresponding with the ignition temperature of dry wood. This temperature estimate is consistent with the indurated nature of the deposit, caused by vapour-phase crystallization and replacement of glassy fragments by zeolite minerals. An interpretation as a primary pyroclastic flow – rather than a lahar – is favoured here for the widespread, axisymmetrical, areal distribution and the relatively high emplacement temperature at considerable distance from the inferred vent area. Enclosed trees provide additional information about timing, rheology and travel direction of the transporting flow (Fig. 4). Nearly complete blow-down of large trees can occur with dynamic overpressures as low as 2 kPa, which can be easily attained by a pyroclastic current with particle volume fraction >0.1 and a lateral speed of a few tens of metres per second (Valentine 1998).

The upward increasing concentration of accretionary lapilli in subunit b2 likely originated at the interface between the lower, dense, avalanche part of the pyroclastic flow and the overriding wet, dilute, ash cloud due to size-sorted ash aggregation and sinking through the moving avalanche (cf. Schumacher and Schmincke 1995) with a possible kinetic sieving effect. Unit c represents deposition by fallout, with a possible surge component, from the turbulent co-ignimbrite ash cloud (Sparks and Walker 1977; Fisher 1979). The gradational b2/c contact and degassing pipes crossing the b2/c unit boundary indicate that deposition of these units was closely spaced in time.

Tractional sedimentation features of unit d point out that pyroclastic surge activity followed a short time break testified by the sharp c/d contact and a thin alluvial horizon in distal areas. Unit e, for its characteristics similar to subunit b2, is interpreted as the deposit of a high-particle-concentration pyroclastic current. Differently from subunits b1 and b2, the erosional d/e contact and the corresponding eruptive break clearly indicate that units d and e originated from distinct flow events. The settling of stagnant fine ash in the atmosphere (unit f) closed the eruption.

From SEM observations, ash-sized scoria particles from unit b are blocky-shaped and poorly vesicular and show hydration cracks. This, consistent with the highly fragmented nature of TTC deposits (except for the basal scoria fall unit) and abundance of minute lithic inclusions and accretionary lapilli, indicates a hydromagmatic character for most of the TTC eruption, except for its initial phase. The absence of vent-derived lithic clasts of the sedimentary substrate and the abundance of minute lava and tuff fragments suggest that the interaction with external water did not involve the deep carbonate aquifer, but a surficial aquifer in the older volcanic terrains.

Petrographic features

Submillimetric euhedral crystals of leucite, scarce clinopyroxene and apatite (referred to as Lc, Cpx and Ap herein) impart sparsely porphyritic textures (<10% by volume of phenocrysts) to juvenile scoria lapilli in TTC. Rare scoria lapilli contain phlogopite (Phl) and Ti-magnetite (Ti-Mt) also. This modal composition is remarkably different from that of highly porphyritic scoria clasts typical of large scoria-flow deposits of the Tuscolano-Artemisio [e.g. the upper flow unit (UFU) of the Villa Senni eruption; Freda et al. 1997], where the Cpx/Lc ratio is much higher (Fig. 5).

Typically, in thin section, leucite in TTC scoria clasts shows concave crystal faces with cuspate angles, due to a more efficient growth at crystal corners, as a clear indication of crystal-melt equilibrium under moderate degree of undercooling. For comparison, in a typical lava of the Tuscolano-Artemisio (the below-mentioned Vallerano lava flow), leucite in the groundmass has cross- or star-like shapes, typical of quench microcrystals formed at high degree of undercooling, whereas millimetre-sized phenocrysts have regular planar faces, indicative of slower growth (Fig. 5). The glassy groundmass of TTC scoria clasts, always altered to form zeolites (see below), shows small, irregularly shaped vesicles, in the amount of ~20 vol.% in units b and e. Loose crystals in the ash fraction of the deposits comprise the same mineral phases found in the scoria clasts.

Microchemical features

The peculiar chemical composition of juvenile scoria clasts from pyroclastic deposits of the Alban Hills (i.e. high Al/Si ratio similar to that of zeolite network) has favoured the more or less complete post-depositional transformation of glass into phillipsite and/or chabazite, with the notable exception of juvenile fiamme in the lower flow unit (LFU) of the Villa Senni eruption (Freda et al. 1997). Due to the lack of fresh scoria of suitable size, the bulk chemical composition of the TTC juvenile material was not determined in the comprehensive work of Trigila et al. (1995). This also discouraged the petrological treatment of these volcanics up to now.

We found glass inclusions in clinopyroxene crystals from scoria clasts that represent the only available unaltered juvenile glass in the TTC (Fig. 6). These are small (up to a few hundred of micrometres) samples of silicate melt trapped during crystal growth and therefore have been chosen as best representative of the melt feeding the TTC eruption (cf. Lowenstern 1995). This analytical approach was favoured by the (a) abundance of uniformly distributed glass inclusions of suitable size, (b) low gas bubble/glass ratio in the inclusions (ranging 0–0.01 by volume), (c) lack of crystalline phases in the inclusions, (d) occurrence of regular, sharp rims without fractures, (e) compositional homogeneity, as indicated by low standard deviation values (Table 1), and (f) lack of

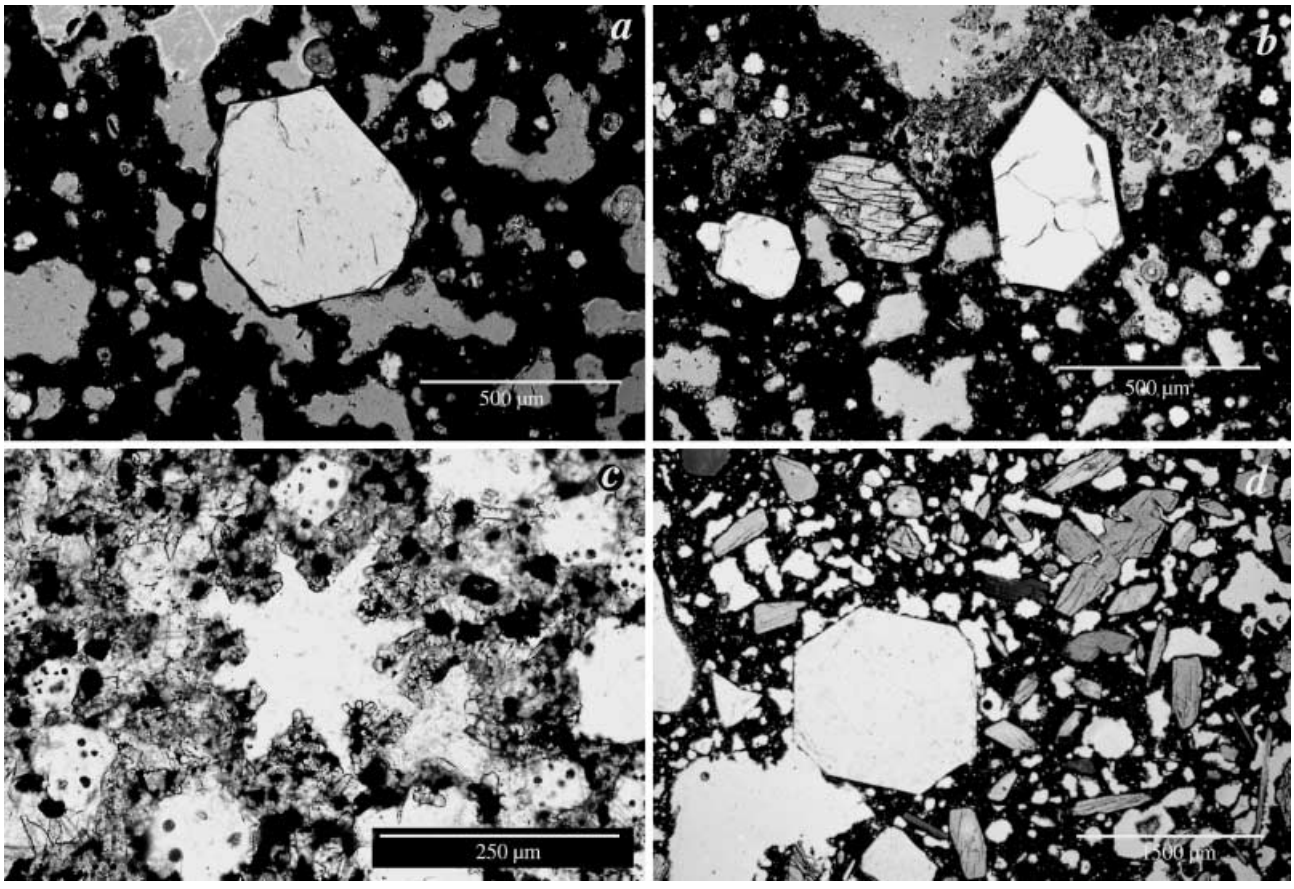

Fig. 5 Photomicrographs of **a, b** leucite phenocrysts in TTC scoria lapilli from subunit b2, **c** star-shaped leucite in the groundmass of *Vallerano* lava flow and **d** leucite phenocryst with planar faces in highly porphyritic scoria clast from the upper flow unit (UFU) of the *Villa Senni* eruption. Plane polarised light. Note *bars* for scale

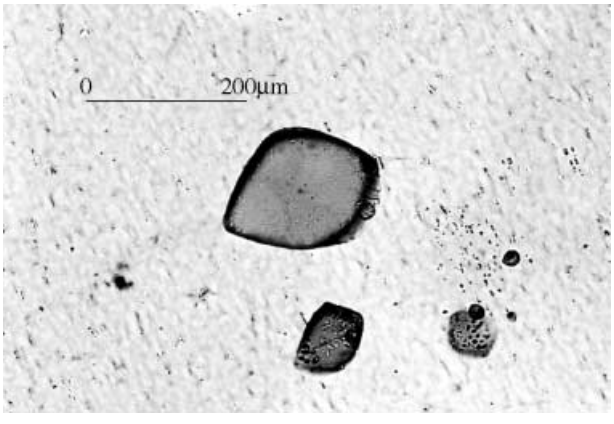

Fig. 6 Photomicrograph of glass inclusions in a clinopyroxene phenocryst from unit e of TTC (Trigoria locality). Plane polarised light

evidence of chemical reactions with the host crystal. Glass inclusions and mineral phases from units a, b and e were analysed by a Cameca SX50 electron microprobe, using the full WD system for major elements and Cr, Ba, Sr, Cl, S and F. The operating conditions (gun at 15 kV and 15 nA, 10-µm beam diameter, 20-s counting time) were maintained constant throughout the analyses. F was analysed using either the PET or PC1 crystals, the obtained values being similar at less than the detection limit. The lack of correlation of 100-(Σoxides+F+Cl) vs either Na_2O (see Fig. 8) or F (not reported), statistically proved by low regression coefficients (R^2=0.0698 and R^2=0.0001, respectively), indicates that the loss of light elements during microprobe analyses was minimized and justifies both the use of Na_2O content in the petrological discussion below, and the application of the equation $H_2O(\pm CO_2)$=100-(Σoxides+F+Cl) for the determination of $H_2O(\pm CO_2)$ contents (cf. Devine et al. 1995) in the glass inclusions.

The chemical compositions of glass inclusions in TTC Cpx (Table 1) plot in the K-foidite field of the total alkali silica (TAS) diagram (Fig. 7), close to LFU glassy fiamme that represent the only previously reported glass compositions of the Alban Hills volcanics; thus, the magma composition erupted at the beginning of the Tuscolano-Artemisio activity phase confirms the compositional field defined by the bulk analyses of lava and pyroclastic products of the Alban Hills (Fornaseri et al. 1963; Trigila et al. 1995). A comparison of the volatile contents of TTC glass inclusions ($H_2O\pm CO_2$=4-5 wt.% on average; Fig. 8) with the ~2 wt.% reported for the glassy fiamme of the Villa Senni LFU (Gaeta 1998), which represent a partially degassed magma, confirms the integrity of the volatile contents in TTC

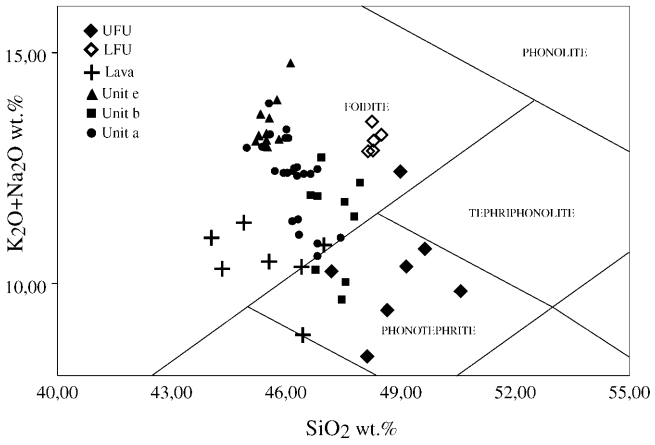

Fig. 7 Plot of TTC glass inclusion analyses in the total alkali silica diagram. The compositions of lower flow unit (LFU) glassy fiamme (data from Gaeta 1998) and upper flow unit (UFU) juvenile scoria clasts (data from Freda et al. 1997) of the *Villa Senni* eruption, the bulk *Vallerano* lava flow (data from Fornaseri et al. 1963; Peccerillo et al. 1984), are also reported for comparison

Table 1 Average microprobe analyses of Trigoria-Tor de' Cenci Tuff (TTC) glass inclusions. *N* number of analyses; σ standard deviation

N	Unit a 23	σ	Unit b 7	σ	Unit e 10	σ
SiO_2	43.34	0.88	44.47	0.45	42.69	0.25
TiO_2	0.91	0.04	0.92	0.05	0.95	0.07
Al_2O_3	16.78	0.44	17.10	0.19	16.30	0.25
Cr_2O_3	0.01	0.02	0.02	0.02	0.01	0.02
FeO_{tot}	8.43	0.30	8.14	0.13	8.37	0.23
MgO	2.42	0.29	2.25	0.26	2.21	0.23
MnO	0.24	0.06	0.23	0.06	0.22	0.06
CaO	9.22	0.40	8.91	0.55	9.44	0.51
SrO	0.26	0.06	0.32	0.14	0.23	0.10
Na_2O	3.35	0.21	3.39	0.40	3.57	0.22
K_2O	8.19	0.75	7.60	0.68	9.04	0.33
BaO	0.47	0.05	0.52	0.06	0.51	0.05
P_2O_5	0.50	0.05	0.45	0.07	0.43	0.16
SO_3	0.98	0.10	1.00	0.12	0.84	0.09
F	0.34	0.06	0.31	0.07	0.44	0.06
Cl	0.13	0.02	0.15	0.02	0.13	0.02
Total	95.57		95.78		95.38	

melt inclusions. Following the classification criterion of Foley et al. (1987), TTC and LFU glasses are not considered primary ultrapotassic rock types, due to MgO<3 wt.%.

The compositions of TTC glass inclusions appear to be unaffected by Na mobility due to secondary processes (allowing the use of Na_2O content as a differentiation index; see below). As normally occurs in potassic volcanics, the alteration of K-foiditic glass to phillipsite and chabazite would have resulted in a negative correlation between H_2O and Na_2O contents, due to high H_2O (15–20 wt.%) and low Na (0–1.5 wt.%) contents in these zeolites, which indeed is not observed in the reported compositions (Fig. 8).

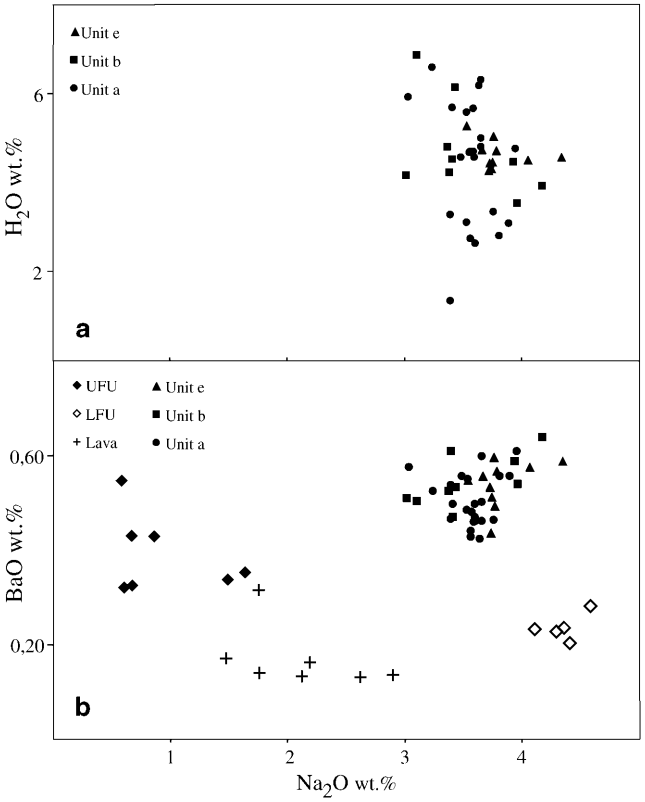

Fig. 8 Plots of **a** H_2O and **b** BaO vs Na_2O for TTC glass inclusions. The same rock types as in Fig. 7 are also reported. The H_2O content was determined by applying the equation $H_2O(\pm CO_2)$= 100-(Σoxides+F+Cl) (cf. Devine et al. 1995). The lack of correlation of H_2O vs Na_2O shows that the loss of light elements during microprobe analyses was minimised and justifies the use of Na_2O content as a differentiation index

Petrological model of the TTC pre-eruptive magma system

The remarkably SiO_2-poor and alkali-rich composition, typical of TTC and the other large-volume pyroclastic units of Tuscolano-Artemisio (Trigila et al. 1995), is not only very rare on a global scale, but also greatly different from trachytes and phonolites characterizing the main pyroclastic deposits of the other volcanic districts of the Quaternary magmatic province of central Italy. In particular, the low Si and high Fe and Ca contents of the TTC glass inclusions contrast strongly with those reported for typical phonolitic Plinian pumice from Somma-Vesuvius (Signorelli et al. 1999).

One of the most distinguishing features of the Alban Hills rock types from those of other districts of the Roman region is the lack of modal plagioclase (Plg) despite high Ca content. This peculiarity originates from the low SiO_2 activity in Alban Hills magmas, which shifts leftward the schematic reaction $CaAl_2SiO_6^{(Cpx)}+SiO_2^{(Liquid)}=CaAl_2Si_2O_8^{(An)}$, resulting in the enlargement of the Cpx stability field and crystallization of Cpx in equilibrium with Lc even in most differentiated magmas. Indeed, the Lc+Cpx assemblage is ubiquitous in the groundmass

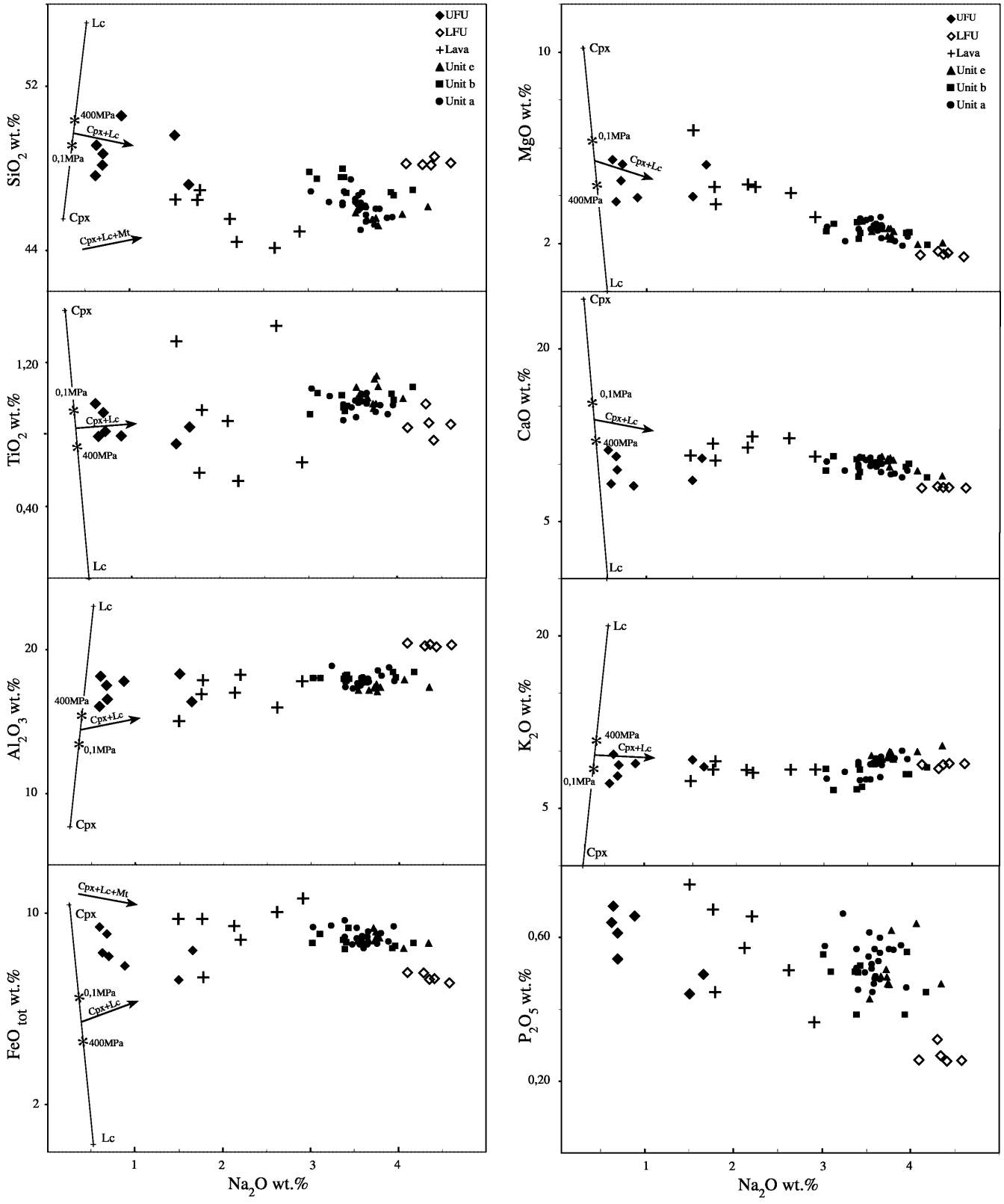

Fig. 9 Variation diagrams of major elements vs Na_2O (on a water-free basis) for TTC glass inclusions. The same rock types as in Figs. 7 and 8 and the Lc-Cpx join, with the position of the binary eutectic at P=0.1 MPa (Bowen and Schairer 1929) and P=400 MPa (Dolfi et al. 1978), are also reported to define a probable line of liquid descent (see text for explanation)

of all lava flows and pyroclastic deposits of the Alban Hills studied up to now (Trigila et al. 1995). Since petrographic evidence of Plg+Lc cotectic crystallization is lacking, the evolution of Alban Hills magmas cannot be adequately modelled in the silica-undersaturated

Table 2 Representative microprobe single-point analyses of TTC minerals. *IN* identification number; *Cpx* clinopyroxene; *Lc* leucite; *Ti-Mt* Ti-magnetite; *Ap* apatite; *Phl* phlogopite

Phase	Cpx	Cpx	Cpx[a]	Cpx	Cpx	Cpx	Lc[a]	Lc	Ti-Mt[a]	Ap[a]	Ap	Phl	Phl
Unit	a	a	b	b	e	e	a	b	b	a	b	a	b
IN	1	9	5	7	15 core	15 rim	10	11	1	4	4	10	10
SiO_2	50.56	45.19	53.97	47.78	48.61	45.69	54.87	55.23	0.32	1.71	1.41	36.20	36.44
Al_2O_3	3.85	7.63	1.60	6.16	4.99	7.33	22.98	22.82	1.08	–	–	15.47	15.82
TiO_2	0.74	1.48	0.35	1.25	0.99	1.39	–	0.02	10.36	–	–	2.99	2.77
Cr_2O_3	–	–	0.14	–	–	–	–	–	–	–	0.01	–	0.01
FeO_{tot}	6.57	10.25	3.17	8.24	8.29	9.33	0.33	0.31	79.83	0.31	0.18	10.46	10.25
MnO	0.10	0.17	0.05	0.10	0.21	0.15	–	–	2.07	–	0.02	0.11	0.13
MgO	13.26	10.11	16.62	11.96	12.66	11.08	–	–	0.88	0.09	0.09	18.74	18.81
CaO	24.36	24.14	24.46	23.61	23.76	23.81	–	–	–	53.97	54.13	–	–
Na_2O	0.32	0.30	0.09	0.29	0.24	0.25	0.52	0.42	–	0.07	0.06	0.21	0.21
K_2O	–	–	–	–	–	–	20.70	20.85	–	–	0.02	9.44	9.28
BaO	–	–	–	–	–	–	0.21	0.06	–	0.10	–	1.65	1.62
SrO	–	–	–	–	–	–	–	–	–	1.00	0.89	–	–
P_2O_5	–	–	–	–	–	–	–	–	–	38.67	39.22	–	–
SO_3	–	–	–	–	–	–	–	–	–	1.54	1.51	–	–
F	–	–	–	–	–	–	–	–	–	2.43	2.38	0.89	0.89
Cl	–	–	–	–	–	–	–	–	–	0.06	0.07	–	–
Total	99.76	99.27	100.45	99.39	99.75	99.03	99.61	99.71	99.54	99.95	99.99	96.16	96.23

[a] Used in mass balance calculations

half of the felsic tetrahedron SiO_2–$NaAlSiO_4$–$KAlSiO_4$–$CaAl_2Si_2O_8$ (phonolite pentahedron; Carmichael et al. 1974). Conversely, petrographic evidence and Cpx crystal chemistry (almost Ca-saturated in the M2 site, with Al_2O_3 contents up to 10–12 wt.% in the groundmass of lava flows) consistently indicate that the liquid line of descent for the Alban Hills products has to be mostly controlled by Lc+Cpx cotectic crystallization.

Crystallization conditions

The TTC melt inclusions are homogeneous in composition (Fig. 9; Table 1), suggesting that magma evolution took place in a system closed to re-filling from the deep source. The mineral assemblage of TTC juvenile scoria clasts containing phenocrysts of Ap+Lc+Cpx and subordinate Ti-Mt and Phl resembles that of the granular holocrystalline lithic inclusions (italite), found in younger eruptive units of Tuscolano-Artemisio, which are considered as the products of the hypabyssal crystallization of foiditic magmas in which phlogopite is a solidus phase (Trigila et al. 1995). The presence of phlogopite thus indicates border zones of the TTC pre-eruptive magma system with relatively high cooling rates and near-solidus temperatures. The F content of TTC phlogopite, as well as the F and SO_3 contents of melt inclusions and apatite primocrysts (Tables 1, 2), indicate $a_{H2O}<1$ in the TTC magma. For comparison, F=0.39 wt.% in experimental phlogopite obtained at P=200 MPa and $a_{H2O}\approx1$ [$H_2O/(H_2O+CO_2)=0.94$] from a UFU scoria starting material (Freda et al. 1997) and F=3.49 wt.% in the Phl from italite inclusions with skarn minerals originating at high P_{CO2} conditions (Gaeta et al. 2000).

The assumption of $a_{H2O}<1$ and the low sensitivity to $P_{(dry)}$ of the binary eutectic Lc-Cpx (Fig. 9) enable us to model the phase relationships in the TTC pre-eruptive magma system on the basis of crystallization experiments performed on leucititic lavas and pyroclasts from Alban Hills at P=0.1 MPa, fO_2=NiNiO buffer and P=200 MPa, $a_{H2O}<1$ (Dolfi and Trigila 1988; Freda et al. 1997). The presence in most TTC scoria clasts of only Ap+Lc+Cpx phenocrysts is compatible with a temperature of 1100–1150°C in the corresponding magma. If higher, we should not have Cpx; if lower, we should also have Ti-Mt phenocrysts, while a lower temperature of 980–1000°C pertains to border zones where the Ap+Lc+Cpx+Ti-Mt+Phl assemblage was forming. The low Fe content of Lc (Table 2) indicates that fO_2 in the inner high-temperature magma zone was comprised between those of the MW and NiNiO buffers (Foley 1985). On the other hand, phlogopite composition indicates fO_2 between those of NiNiO and MH buffers for the low-temperature magma border zone (Gaeta et al. 2000). Finally, the $Lc_{41}Cpx_{59}$ proportion in the fractionating assemblage of the TTC pre-eruptive magma system (Table 3; see below) indicates P<200 MPa (with $a_{H2O}<1$), consistent with the depth of the old Tuscolano-Artemisio magma chamber inferred from seismic tomography (Chiarabba et al. 1997).

Liquid line of descent

Considering the significant differences in crystal content of TTC relative to UFU juvenile scoria clasts, it could be argued that corresponding pre-eruptive melts should have been different in composition. In contrast, the composition of TTC glasses matches that of LFU glassy fiamme, which are considered as representative of the Villa Senni pre-eruptive melt (Freda et al. 1997; Gaeta 1998). Furthermore, it is not possible to distinguish in the TAS

Table 3 Results of mass balance calculations. *FeCaTS* FeCa-Tschermak; *Di* diopside; *Lc* leucite; *Cpx* clinopyroxene; *LFU* lower flow unit

Starting composition	Final composition	Σ (residual)^2	Total solid fractionated (%)	FeCaTS/(FeCaTS+Di) (%)	Lc/(Lc+Cpx) (%)	Ti-magnetite (%)	Apatite (%)
Vallerano lava[a]	Unit a (TTC)	0.533	44	40[c]	41	1.9	0.4
Vallerano lava[a]	LFU (*Villa Senni*)[b]	0.484	58	36[d]	42	3.8	1.4

[a] Average of data from Fornaseri et al. (1963)
[b] Average of data from Gaeta (1998)
[c] Cpx A in Table 4
[d] Cpx B in Table 4

diagram (Fig. 7) which is the most differentiated relative to the bulk compositions of the Vallerano lava type (the first large lava flow following the TTC eruption) or the highly porphyritic UFU scoria clasts. The usual SiO_2 enrichment in residual melts with ongoing differentiation is not observed in the case of the Alban Hills, rendering the identification of a clear liquid line of descent ambiguous. For this reason, the TAS diagram is not suitable to represent the evolution of these magmas (Trigila et al. 1995).

In this work we use the Na_2O content as a possible differentiation index for the Tuscolano-Artemisio volcanics, based on the following petrographic evidence in the lava flows: (a) primary nepheline is commonly present in the groundmass; (b) Cpx in the groundmass and Cpx phenocryst rims are rich in the aegirine component; and (c) Lc in the groundmass and Lc phenocryst rims are Na_2O-rich (Trigila et al. 1995). We recall that all glasses analysed in this work have no evidence of post-depositional Na leaching (Fig. 8). In Fig. 9 the variation diagrams of major elements vs Na_2O are reported for TTC, Villa Senni and Vallerano rock types, aiming at reconstructing a probable line of liquid descent.

In several diagrams (i.e. TiO_2, Al_2O_3, MgO, CaO, K_2O vs Na_2O), the Vallerano lava and TTC and LFU glass compositions define a residual liquid trend, which likely represents a liquid line of descent, mostly controlled by Lc+Cpx removal from a parent magma corresponding to the Vallerano lava. In addition, the trends of SiO_2, FeO and P_2O_5 (Fig. 9) rule out a possible UFU composition for the parent magma and indicate that the actual extracted assemblage, driving the compositional evolution from the Vallerano lava-type to TTC (or LFU), comprised small amounts of Ti-Mt and Ap.

The above crystal-liquid fractionation hypothesis has been tested by mass balance calculations (Table 3). Both a Cpx rich in diopside component (Table 2) and a Cpx of $(CaAlAlSiO_6)_{60}$-$(CaFeAlSiO_6)_{40}$ composition (Table 4) have been included in the fractionating assemblage to provide a further petrological test to the hypothesis that the cotectic crystallization of Lc+$CaAlAlSiO_6$ replaces that of Lc+Plg at low SiO_2 activity. Least squares residuals <1 (Table 3) used as the main constraint to verify the consistency of mass balance calculations confirm that it is possible to obtain a melt with a composition similar to TTC (Table 1) by subtracting a Lc+Cpx+Ti-Mt+Ap solid assemblage from a parent composition corresponding to the Vallerano lava type. The Lc/(Lc+Cpx) ratio in the fractionated assemblage (Table 3) plots in the interval between the Lc-Cpx cotectic proportions at P=0.1 MPa ($Lc_{38}Cpx_{62}$) and P=400 MPa ($Lc_{50}Cpx_{50}$; Fig. 9; Bowen and Schairer 1929; Dolfi et al. 1978), supporting the petrological reality of the foregoing mass balance calculations; these are consistent with the calculated FeCaTS amount relative to the total fractionated Cpx (Table 3) and the Cpx chemistry in lava and pyroclastic products of Tuscolano-Artemisio, in which up to one-fifth of tetrahedral Si sites may be substituted by Al (Baldridge et al. 1981; Aurisicchio et al. 1988). A further support is the occurrence of Ap+Lc+Cpx+Ti-Mt-bearing hypabyssal lithic inclusions with suitable Cpx/Lc ratio (italite; Trigila et al. 1995) in the overlying Palatino unit and above.

Table 4 Theoretical Cpx compositions used in and obtained from mass balance calculations. *FeCaTS* FeCa-Tschermak; *Cpx* clinopyroxene

	FeCaTS	Cpx A	Cpx B
SiO_2	24.91	42.26	43.43
TiO_2	–	0.21	0.22
Al_2O_3	25.36	11.10	10.15
Fe_2O_3	26.48	10.42	9.36
FeO	–	2.06	2.18
MgO	–	9.94	10.60
MnO	–	0.03	0.03
CaO	23.25	23.93	23.97
Na_2O	–	0.05	0.06
Total	100.00	100.00	100.00

It is apparent that, starting from a similar magma composition, by fractionating the same mineral phases, the resulting LFU rock type is more differentiated than TTC (Fig. 9; Table 3) and the most evolved of the entire Tuscolano-Artemisio phase, consistent with the occurrence of Ba-sanidine in LFU fiamme (Gaeta 1998). The high Ba content of LFU sanidine accounts for the higher Ba content of LFU relative to TTC (Fig. 8). In this framework, the UFU rock type is thought to represent a cumulus-enriched magma, consistent with the model of Freda et al. (1997).

The foregoing fractionation scheme is compatible with the observed mineral assemblage of TTC scoria clasts; however, the observed low crystal amount in TTC scoria clasts seem to conflict with that from mass balance calculations, with that obtained experimentally at T<1150°C (Lc+Cpx±Ti-Mt>20% by volume; Dolfi and Trigila 1988; Trigila et al. 1995), and with the above re-

ported cotectic proportions in the Lc-Cpx system at P=400 and P=0.1 MPa. This can be explained by assuming that the TTC pre-eruptive magma system was zoned in crystalline/melt and Lc/Cpx proportions, despite homogeneous melt composition (except for possible gradients of volatile activities).

This zonation recalls that proposed for the Villa Senni eruption, where the LFU derived from the inner, crystal-poor part of the magma reservoir and the UFU from the crystal-rich margins (Freda et al. 1997). It is consistent with the common occurrence of italites and ultramafic cumulates in the upper eruptive units of the Tuscolano-Artemisio (Trigila et al. 1995; Gaeta et al. 2000). Possible causes of zoning include the a_{H2O} gradient due to decarbonation of country rocks (cf. Freda et al. 1997; Gaeta et al. 2000) and the significant Cpx-Lc and Cpx-melt density contrasts.

Discussion and conclusion

The TTC deposits, except for the common occurrence of a basal fallout bed, differ from the typical massive, coarse-grained, crystal-rich scoria-flow deposits of the Tuscolano-Artemisio phase (Pozzolane Rosse, Pozzolane Nere and UFU; Trigila et al. 1995). The TTC peculiarities, which we attribute to its hydromagmatic origin, are: relatively complex deposit architecture, defined by alternating massive and stratified divisions; notably fine grain size, due to the lack of coarse lapilli and blocks; and abundance of accretionary lapilli. Hydromagmatism dominated the more recent volcanic activity of the Alban Hills, the so-called final hydromagmatic phase (Fig. 2; De Rita et al. 1988), but the scale of the TTC event remains unparalleled. Other differences are: scarcely porphyritic juvenile scoria clasts; the paucity of lithic inclusions from the sedimentary substrate and the lack of italite inclusions; and the composition of the volatile phase, rich in unusual components such as S and F.

In general, the melts erupted through the Tuscolano-Artemisio activity phase are remarkably homogeneous in composition (the Villa Senni eruption, the last large explosive event of this phase, took place 200 ka after the TTC). In agreement with Freda et al. (1997) and Gaeta et al. (2000), it is likely that the pre-eruptive magma system feeding large explosive eruptions has been invariably controlled by fractionation of Lc+Cpx+accessories under $a_{H2O}<1$ conditions during the entire Tuscolano-Artemisio activity. Mass balance calculations bearing on the liquid line of descent of Fig. 9 indicate that the degree of crystallization and consequent volatile oversaturation in TTC magma was significantly lower than in the Villa Senni case.

In contrast to the magmatic eruptions of Tuscolano-Artemisio, the juvenile volatile exsolution related to crystallization (cf. the role of H_2O and CO_2 on the Villa Senni eruption; Freda et al. 1997) does not seem to be the main mechanism driving the TTC eruption, and we think that hydromagmatism acted in this respect. We note that the $H_2O \pm CO_2$ contents of the TTC melt were probably below saturation conditions at the inferred depth of the magma chamber (Trigila et al. 1995; Freda et al. 1997; Carroll and Blank 1997). Indeed, those eruptions were controlled by CO_2 oversaturation (e.g. Villa Senni) and hydromagmatism was inhibited. To assess the role of unusually high F and S contents in the juvenile volatile phase of TTC on the eruptive mechanism and possible influence on interaction with external water, future investigation would be required.

To explain the explosive capability of the TTC magma at the onset of the eruption (unit a), it seems likely that the sudden stress release linked to a regional earthquake may have played a role in triggering the violent volatile exsolution (Brodsky et al. 1998). Examples of normal-faulting earthquakes closely associated with eruptions and/or volcanic inflation are widely reported in the recent literature (see Nostro et al. 1998 for a review). Nostro et al. (1998) interpret the relationship among Vesuvius eruptions and neighbouring Apennine earthquakes as a consequence of elastic stress transfer, where small stress changes can promote eruptive events when the Vesuvius magma body is close to failure. We believe that such a triggering mechanism had a great potential to act in the case of the Roman volcanoes in the context of extensional tectonics along the NW–SE faults on the Tyrrhenian margin of Italy.

The paucity of lithic fragments in unit a suggests limited erosion of stable conduit walls during the sustained eruption column, magmatic phase. Possible choked flow conditions in the conduit and interaction with external water due to conduit wall failure eventually led to overpressured hydromagmatic blast originating unit b. The volcanic nature of lithic inclusions in unit b and subsequent units suggests that hydromagmatic fragmentation occurred at a shallow level, due to interaction with an aquifer located in the older Alban Hills volcanic cover, which was likely to exist below the vent area. The possible encounter of the rising magma with a surficial aquifer is in good agreement with the radiometric age of the TTC eruption, corresponding to a phase of high sea-level stand (Bassinot et al. 1994). At that time, the continental environment where the eruption took place was likely characterized by the forested slopes of the growing volcano, surrounded by swampy lowlands (as testified by the finding of reed remnants in the TTC) and nearby coastal areas. The large availability of water could explain the dominant hydromagmatic character of the eruption till its end.

Evidence of tapping of shallow/inner portions of the magma chamber, without the involvement of the deep mafic cumulates and highly crystallized margins of the magma reservoir, is provided by the lack of corresponding hypabyssal inclusions, which typically occur in other pyroclastic flow deposits of the Tuscolano-Artemisio phase and were likely to have controlled magma evolution in the TTC case also.

The pre-eruptive crystallization conditions allow the TTC magma chamber depth to be constrained at

P=100–200 MPa (~3–6 km), as also required by the onset of a Plinian-type column in the early phase of the eruption. The inferred depth is comparable to that of the following large eruptions of Tuscolano-Artemisio and consistent with a magma reservoir located within the carbonate substrate (Freda et al. 1997; Chiarabba et al. 1997).

In comparison with erupted low-SiO_2 magmas all over the world, the TTC documents energetic explosive activity and large volume of products from a mafic magma. Indeed, the outlined eruptive scenario and the magnitude of pyroclastic currents are comparable with those of more usual silicic events, although the composition of TTC (and, in general, of highly explosive magmas of Tuscolano-Artemisio), is unique on a planetary scale and represents an exception even within the Quaternary potassic volcanoes of central Italy (where the largest Plinian and pyroclastic-flow-forming events are mostly trachytic to phonolitic in composition).

The anomalous behaviour of the magma system of the Alban Hills, relative to nearby volcanic districts of the Tyrrhenian margin, is still an unsolved problem. On the other hand, the Alban Hills rock types share their main peculiarities, i.e. the low SiO_2 activity (and consequent lack of feldspars) and the high Ca activity (and consequent presence of magmatic calcite in the lava flows), with the intra-Apennine small volcanic centres of Cupaello and Polino (Peccerillo 1998). Even if a carbonate substrate is present below the other potassic districts, the Meso-Cenozoic carbonate successions underlying the Alban Hills and the intra-Apennine centres are considerably overthickened. It is therefore suggested that the peculiar evolution of Alban Hills magmatism was controlled by the deeper and more prolonged interaction of the primary magmas with overthickened carbonate country rocks under $a_{H2O}<1$ crystallization conditions.

Acknowledgements We are grateful to M. Ort and S. de Silva for their thorough reviews, and to M. Carroll for reading a previous version of the paper. We acknowledge M. Serracino, of the Centro di Studio per il Quaternario e l'Evoluzione Ambientale, CNR, Rome, for technical assistance in microprobe analyses. M. Albano, L. Di Pietro and M. Salvati are also acknowledged for drawing some figures.

References

Aurisicchio C, Federico M, Gianfagna A (1988) Clinopyroxene chemistry of the high-potassium suite from the Alban Hills, Italy. Mineral Petrol 39:1–19

Baldridge WS, Carmichael ISE, Albee AL (1981) Crystallization paths of leucite-bearing-lavas: examples from Italy. Contrib Mineral Petrol 76:321–335

Bassinot FC, Labeyrie LD, Vincent E, Quidelleur X, Shackleton NJ, Lancelot Y (1994) The astronomical theory of climate and the age of the Brunhes-Matuyama magnetic reversal. Earth Planet Sci Lett 126:91–108

Boni C, Bono P, Lombardi S, Mastrorillo L, Percopo C (1995) Hydrogeology, fluid geochemistry and thermalism. In: Trigila R (ed) The Volcano of the Alban Hills. SGS, Rome, pp 221–242

Bourdier JL, Abdurachman EK, Voight B (1997) Flow-surge facies relationships and nuée ardente emplacement at Merapi volcano. Abstr IAVCEI Gen Ass Puerto Vallarta, Mexico, p 82

Bowen NL, Schairer JF (1929) The system: leucite-diopside. Am J Sci 18:301–312

Brodsky EE, Sturtevant B, Kanamori H (1998) Earthquakes, volcanoes, and rectified diffusion. J Geophys Res 103:827–838

Carmichael ISE, Turner FJ, Verhoogen J (1974) Igneous petrology. McGraw-Hill, New York, pp 1–739

Carroll MR, Blank JG (1997) The solubility of H_2O in phonolitic melts. Am Mineral 82:549–556

Chiarabba C, Amato A, Delaney PT (1997) Crustal structure, evolution, and volcanic unrest of the Alban Hills, Central Italy. Bull Volcanol 59:161–170

De Rita D, Funiciello R, Parotto M (1988) Carta Geologica del Complesso Vulcanico dei Colli Albani. Scala 1:50,000. CNR Rome

De Rita D, Faccenna C, Funiciello R, Rosa C (1995) Stratigraphy and volcano-tectonics. In: Trigila R (ed) The volcano of the Alban Hills. SGS, Rome, pp 31–71

De Rita D, Funiciello R, Corda L, Sposato A, Rossi U (1993) Volcanic units. In: Di Filippo M (ed) Sabatini Volcanic Complex. CNR, Rome, pp 33–79

Devine JD, Gardner JE, Brack HP, Layne GD, Rutherford MJ (1995) Comparison of microanalytical methods for estimating H_2O contents of silicic glasses. Am Mineral 80:319–328

Dolfi D, Trigila R (1988) Chemical relations between clinopyroxenes and coexisting glasses obtained from melting experiments on alkaline basic lavas. Rend Soc Ital Mineral Petrol 43:1101–1110

Dolfi D, Hamilton DL, Trigila R (1978) The system $KAlSi_2O_6$–$CaMgSi_2O_6$ at 4 and 12 kilobars. Progr Exp Petrol 4:23–24

Faccenna C, Funiciello R, Mattei M (1994) Late Pleistocene N–S shear zones along the Latium Tyrrhenian margin: structural characters and volcanological implications. Boll Geof Teor Appl 36:507–522

Fisher RSV (1979) Models for pyroclastic surges and pyroclastic flows. J Volcanol Geotherm Res 6:305–318

Foley SF (1985) The oxidation state of lamproitic magmas. Tschermaks Mineral Petrol Mitteil 34:217–238

Foley SF, Venturelli G, Green DH, Toscani L (1987) The ultrapotassic rocks: characteristics, classification, and constraints for petrogenetic models. Earth Sci Rev 24:81–134

Fornaseri M, Scherillo A, Ventriglia U (1963) La regione vulcanica dei Colli Albani. Vulcano Laziale. CNR, Rome, pp 1–561

Freda C, Gaeta M, Palladino DM, Trigila R (1997) The Villa Senni Eruption (Alban Hills, Central Italy): the role of H_2O and CO_2 on the magma chamber evolution and on the eruptive scenario. J Volcanol Geotherm Res 78:103–120

Funiciello R, Parotto M (1978) Il substrato sedimentario nell'area dei Colli Albani: considerazioni geodinamiche e paleogeografiche sul margine tirrenico dell'Appennino centrale. Geol Romana 17:233–287

Gaeta M (1998) Petrogenetic implications of Ba-sanidine in the Lionato Tuff (Colli Albani Volcanic District, Central Italy). Mineral Mag 62:697–701

Gaeta M, Fabrizio G, Cavarretta G (2000) F-phlogopites in the Alban Hills Volcanic District (Central Italy): indications regarding the role of volatiles in magmatic crystallization. J Volcanol Geotherm Res 99:179–193

Karner DB, Renne P (1998) $^{40}Ar/^{39}Ar$ geochronology of Roman volcanic province tephra in the Tiber River valley: age calibration of middle Pleistocene sea-level changes. Geol Soc Am Bull 110:740–747

Karner DB, Marra F, Renne P (2001a) The history of the Monti Sabatini and Alban Hills volcanoes: groundwork for assessing volcanic-tectonic hazards for Rome. J Volcanol Geotherm Res 107:185–219

Karner DB, Marra F, Florindo F, Boschi E (2001b) Pulsed uplift estimated from terrace elevations in the coast of Rome: evidence for a new phase of volcanic activity? Earth Planet Sci Lett 188:135–148

Locardi E, Lombardi G, Funiciello R, Parotto M (1977) The Main volcanic groups of Latium (Italy): relations between structural evolution and petrogenesis. Geol Romana 15:279–300

Lowenstern JB (1995) Applications of silicate-melt inclusions to the study of magmatic volatiles. In: Thompson JFH (ed) Magmas, fluids, and ore deposits. Mineral Assoc Can Short Course Series 23:71–99

Malinverno A, Ryan WBF (1986) Extension in the Tyrrhenian sea and shortening in the Apennines as results of arc migration driven by sinking of the lithosphere. Tectonics 5:227–245

Marra F (2001) Strike-slip faulting and block rotation: a possible triggering mechanism for lava flows in the Alban Hills. J Struct Geol 23:127–141

Marra F, Rosa C (1995) Stratigrafia e assetto geologico dell'area romana. Mem Descr Carta Geol d'It 50:49–118

Marra F, Carboni MG, Di Bella L, Faccenna C, Funiciello R, Rosa C (1995) Il substrato plio-pleistocenico nell'Area Romana. Boll Soc Geol Ital 114:195–214

Marra F, Rosa C, De Rita D, Funiciello R (1998) Stratigraphic and tectonic features of the Middle Pleistocene sedimentary and volcanic deposits in the area of Rome (Italy). Quaternary Int 47/48:51–63

Nostro C, Stein RS, Cocco M, Belardinelli ME, Marzocchi W (1998) Two-way coupling between Vesuvius eruptions and southern Apennine earthquakes, Italy, by elastic stress transfer. J Geophys Res 103:487–505

Palladino DM, Agosta E (1997) Pumice fall deposits of the western Vulsini Volcanoes (central Italy). J Volcanol Geotherm Res 78:77–102

Patacca E, Sartori R, Scandone P (1991) Tyrrhenian Basin and Apenninic arcs: kinematic relations since late Tortonian times. Mem Soc Geol Ital 45:425–451

Peccerillo A (1998) Relationships between ultrapotassic and carbonate-rich volcanic rocks in central Italy: petrogenetic and geodynamic implications. Lithos 43:267–279

Peccerillo A, Poli G, Tolomeo L (1984) Genesis, evolution and tectonics significance of K-rich volcanics from the Alban Hills (Roman Comagmatic Region) as inferred from trace element geochemistry. Contrib Mineral Petrol 86:230–240

Pyle DM (1989) The thickness, volume and grainsize of tephra fall deposits. Bull Volcanol 51:1–15

Schumacher R, Schmincke HU (1995) Models for the origin of accretionary lapilli. Bull Volcanol 56:626–639

Serri G, Innocenti F, Manetti P, Tonarini S, Ferrara G (1991) Il magmatismo neogenico-quaternario dell'area tosco-laziale-umbra: implicazioni sui modelli di evoluzione geodinamica dell'Appennino settentrionale. Studi Geol Camerti Vol Spec 1:429–463

Signorelli S, Vaggelli G, Romano C (1999) Pre-eruptive volatile (H_2O, F, Cl and S) contents of phonolitic magmas feeding the 3550-year old Avellino eruption from Vesuvius, southern Italy. J Volcanol Geotherm Res 93:237–256

Sparks RSJ, Walker GPL (1977) The significance of vitric-enriched air-fall ashes associated with crystal-enriched ignimbrites. J Volcanol Geotherm Res 2:329–341

Trigila R, Agosta E, Currado C, De Benedetti AA, Freda C, Gaeta M, Palladino DM, Rosa C (1995) Petrology. In: Trigila R (ed) The Volcano of the Alban Hills. SGS, Rome, pp 95–165

Valentine GA (1998) Damage to structures by pyroclastic flows and surges, inferred from nuclear weapons effects. J Volcanol Geotherm Res 87:117–140

Walker GPL (1973) Explosive volcanic eruptions: a new classification scheme. Geol Rundsch 62:431–446

Washington HS (1906) The Roman Comagmatic Region. Carnegie Inst Washington Yearb 56:206–214